HHS Public Access

Author manuscript

Nat Cell Biol. Author manuscript; available in PMC 2015 October 01.

Published in final edited form as:

Nat Cell Biol. 2015 April ; 17(4): 500–510. doi:10.1038/ncb3111.

Cellular energy stress induces AMPK-mediated regulation of YAP and the Hippo pathway

Jung-Soon Mo[1], **Zhipeng Meng**[1], **Young Chul Kim**[1], **Hyun Woo Park**[1], **Carsten Gram Hansen**[1], **Soohyun Kim**[1], **Dae-Sik Lim**[2], and **Kun-Liang Guan**[1,*]

[1]Department of Pharmacology and Moores Cancer Center, University of California, San Diego, La Jolla, CA 92093, USA

[2]National Creative Research Initiatives Center, Department of Biological Sciences, Korea Advanced Institute of Science and Technology, Daejeon, Republic of Korea

Abstract

YAP (Yes-associated protein) is a transcription co-activator in the Hippo tumor suppressor pathway and controls cell growth, tissue homeostasis, and organ size. YAP is inhibited by the kinase Lats, which phosphorylates YAP to induce its cytoplasmic localization and proteasomal degradation. YAP induces gene expression by binding to the TEAD family transcription factors. Dysregulation of the Hippo-YAP pathway is frequently observed in human cancers. Here we show that cellular energy stress induces YAP phosphorylation, in part due to AMPK-dependent Lats activation, thereby inhibiting YAP activity. Moreover, AMPK directly phosphorylates YAP S94, a residue essential for the interaction with TEAD, thus disrupting the YAP-TEAD interaction. AMPK-induced YAP inhibition can suppress oncogenic transformation of Lats-null cells with high YAP activity. Our study establishes a molecular mechanism and functional significance of AMPK in linking cellular energy status to the Hippo-YAP pathway.

INTRODUCTION

The Hippo pathway was originally discovered in *Drosophila*[1] to regulate organ size and is highly conserved in higher eukaryotes[2]. Core components of the mammalian Hippo pathway include MST1/2 and Lats1/2 kinases and their downstream effectors, YAP and TAZ transcription co-activators[3]. In response to unfavorable growth conditions, MST1/2 phosphorylate and activate Lats1/2, which in turn phosphorylate and inhibit YAP/TAZ. The Lats-dependent phosphorylation of YAP/TAZ promotes their binding to 14-3-3, resulting in cytoplasmic localization and functional inactivation[4–6]. Moreover, phosphorylated

*To whom correspondence should be addressed: kuguan@ucsd.edu.

AUTHOR CONTRIBUTION

J-S.M. and K.-L.G., designed the experiments, analyzed data and wrote the paper. J-S.M. performed the experiments with assistance from Z.M., Y.C.K., H.W.P., C.G.H. and S.K. D-S.L. established the Lats knockout MEFs. All authors discussed the results and commented on the manuscript.

COMPETING FINANCIAL INTERESTS

The authors declare no competing financial interests.

YAP/TAZ are targeted for ubiquitination and degradation[7, 8]. The Hippo pathway thus suppresses tumorigenesis by limiting the activity of YAP/TAZ[9–11]. YAP/TAZ activity must be strictly regulated for tissue/organs to reach and maintain proper size[2, 3, 12–14]. YAP/TAZ can promote cell proliferation and inhibit apoptosis; abnormal activation of YAP/TAZ is frequently found in human cancers[15, 16]. However, the function of YAP in human cancer is complex and could be cell-type-dependent. For instance, YAP could function as a tumor suppressor in some cell types, such as hematological cancers, by inducing apoptosis in response to DNA damage[17–19].

Recent studies have revealed a large number of extra- and intracellular signals that modulate YAP/TAZ activity. For example, cell density/cell contact strongly suppresses YAP activity concomitantly with increased Lats kinase activity[4], which may be mediated by tight junctions and adherent junctions[20, 21]. Diffusible hormones, such as lysophosphatidic acid and epinephrine acutely regulate YAP activity (either stimulatory or inhibitory) via G-protein coupled receptor (GPCR)[22–25]. Furthermore, mechanic stress has been shown to regulate YAP activity[26–28]. These signals might all act through alteration of actin dynamics to modulate Lats kinase activity and YAP function.

In this study, we discovered that YAP is inhibited by cellular energy stress. AMPK is a key cellular energy sensor activated by increasing AMP levels and functions to coordinate cell growth with energy availability. We show that AMPK can inhibit YAP by two mechanisms: directly via phosphorylation of YAP S94, and indirectly via activation of the Lats kinase. This work therefore reveals molecular insights of Hippo-YAP regulation by cellular energy status.

RESULTS

Cellular energy starvation induces YAP phosphorylation and inactivation

Cell growth is an energy-consuming process and must be coordinated with cellular energy status. Given the key function of YAP in cell growth regulation, we investigated whether YAP is regulated by energy stress. Glucose starvation strongly induced YAP phosphorylation as determined by mobility shift on a phos-tag gel (Fig. 1a). Previous studies have shown that Lats phosphorylates YAP on five serine residues and phosphorylation of S127 is critical for the interaction between YAP and 14-3-3, which sequesters YAP in the cytoplasm[4]. Glucose starvation induced YAP S127 phosphorylation (Fig. 1a), suggesting that cellular energy stress inhibits YAP. AMPK is a key cellular energy sensor. As expected, glucose starvation activated AMPK as indicated by the increased phosphorylation of the activation loop T172 in AMPKα (Fig. 1a)[29]. 2-deoxy-D-glucose (2-DG) is a nonmetabolizable glucose analog that can inhibit normal glucose metabolism therefore inducing cellular energy stress. Addition of 2-DG activated AMPK as indicated by the increased phosphorylation of acetyl-CoA Carboxylase (ACC), an AMPK substrate, and also induced YAP phosphorylation (Fig. 1b). The effect of 2-DG on YAP phosphorylation was more robust in low-glucose conditions. We tested YAP phosphorylation using a similar concentration of sorbitol and found that the effect of 2-DG was specific, excluding a possible osmotic effect (Supplementary Fig.1a). 2-DG increased the phosphorylation of AMPKα and YAP in a dose- and time dependent manner (Supplementary Fig. 1b, c).

Notably, 2-DG also induced a TAZ mobility shift, indicating that 2-DG also increased TAZ phosphorylation. It is worth noting that ACC phosphorylation was more sensitive to 2-DG treatment than YAP phosphorylation (Fig.1b), consistent with the distinct cellular functions of ACC (fatty acid synthesis and energy storage) and YAP (cell growth and survival). One may speculate that fatty acid synthesis should be inhibited prior to growth inhibition and apoptosis. Thus, ACC could be inhibited under mild energy stress whereas more severe energy stress is required to inhibit YAP. Energy stress-induced YAP phosphorylation was also observed in myoblast C2C12, mammary epithelial MCF10A, and the cervical cancer HeLa cell lines (Supplementary Fig. 1d–f).

A major role of YAP phosphorylation is to promote its cytoplasmic sequestration[4]. Immunofluorescence staining of endogenous YAP revealed that 2-DG treatment decreased nuclear and increased cytoplasmic YAP staining (Fig. 1c). Numerous transcription factors have been implicated to be YAP targets; in particular, the TEAD family has been most convincingly shown to mediate biological functions of YAP[12, 13, 30–32]. Consistent with the cytoplasmic YAP localization, 2-DG blocked the interaction between YAP and TEAD (Fig. 1d). Glucose starvation also diminished YAP-TEAD interaction (Supplementary Fig. 1g). These observations link cellular energy stress to YAP inhibition. To further confirm the negative regulation of YAP by cellular energy stress, we measured YAP target gene expression and found that 2-DG treatment significantly decreased the expression of TEAD target genes, CTGF and CYR61 (Fig. 1e)[3]. Collectively our data suggest that cellular energy stress inhibits YAP and TAZ activity.

Energy stress activates Lats kinase

The increase of YAP S127 phosphorylation indicates that Lats kinase activity is enhanced by energy stress (Fig. 1a). Phosphorylation of S909 and T1079 in Lats1 positively correlate with Lats activity[33, 34]. We therefore monitored S909 and T1079 phosphorylation in endogenous Lats1 in response to energy stress. 2-DG treatment significantly increased phosphorylation of both residues in immunoprecipitated Lats1 (Fig. 1f). In addition, we directly measured Lats1 kinase activity through an *in vitro* kinase assay using recombinant YAP as a substrate. Lats1 immunoprecipitated from glucose-starved HEK293A cells displayed a significantly higher kinase activity towards YAP (Fig. 1g). Next, we investigated the function of MST in energy stress-induced YAP phosphorylation. Overexpression of wild-type MST2 had a minor effect on 2-DG-induced YAP phosphorylation whereas the MST2 kinase-inactive (MST2-KR) mutant partially blocked the YAP mobility shift (Supplementary Fig. 2a). However, 2-DG did not activate MST, as the activation loop phosphorylation of MST (T183) was not increased (Supplementary Fig. 2b). Thus, we conclude that cellular energy stress activates Lats activity and promotes YAP phosphorylation and inhibition which might have a role in cell growth suppression in response to energy starvation.

AMPK is required for energy starvation-induced YAP phosphorylation

AMPK directly monitors cellular ATP and AMP levels and regulates cell metabolism and growth in response to cellular energy status[29]. We investigated the role of AMPK in YAP regulation by comparing AMPKα wild-type (WT) and AMPKα α double-knockout (DKO)

mouse embryonic fibroblasts (MEFs) that lack the two AMPK catalytic alpha subunits (Supplementary Fig. 3a). Notably, 2-DG treatment failed to induce YAP mobility shift in the AMPKα DKO MEFs, indicating a critical role of AMPKα in YAP regulation by energy stress (Fig. 2a). Treatment with lambda phosphatase (λ-PPase) abolished the 2-DG-induced YAP mobility shift (Supplementary Fig. 3b). These data indicate that cellular energy stress induces YAP phosphorylation in an AMPK-dependent manner.

We next determined whether AMPK is sufficient to induce YAP phosphorylation. Expression of WT AMPKα1 or AMPKα2, but not the DN mutant, induced significant YAP phosphorylation as indicated by the altered mobility shift on a phos-tag gel (Fig. 2b), suggesting that AMPK can induce YAP phosphorylation. Moreover, 2-DG could activate Lats1 in AMPKα WT MEFs, but 2-DG-induced Lats phosphorylation was partially compromised in the AMPKα DKO MEFs (Fig. 2c). These data suggest that AMPK relays, at least partly, the energy stress signal to Lats activation. Consistent with a role in YAP inhibition, we confirmed that AMPK co-transfection disrupted the YAP-TEAD interaction (Fig. 2d) and suppressed TEAD-luciferase reporter activity (Fig. 2e). Furthermore, the AMPK-DN increased reporter activity, consistent with the notion that AMPK-DN interferes with endogenous AMPK function in a dominant-negative fashion..

Metformin, a widely prescribed drug for type II diabetes[35], activates AMPK, inhibits cell growth and reduces tumor incidence[36, 37]. Most *in vitro* studies use doses of metformin significantly higher than the therapeutic levels of plasma metformin [38]. We found that metformin treatment increased AMPK activity and YAP phosphorylation (Fig. 2f). Metformin also increased TAZ phosphorylation. Aminoimidazole carboxamide ribonucleotide (AICAR) is a well-known AMPK activator [29]. Similar to metformin, AICAR induced YAP and TAZ phosphorylation (Supplementary Fig. 3c). YAP S127 phosphorylation was decreased by AICAR treatment, indicating a possible disconnection between AMPK activation and Lats activation under this condition. A YAP-TEAD co-immunoprecipitation experiment revealed that AICAR reduced the interaction between YAP and TEAD (Fig. 2g). Metformin and AICAR treatments also decreased the expression of YAP-TEAD target genes Ctgf and Cyr61 (Fig. 2h). The stronger inhibitory effects of AICAR on YAP target genes are consistent with the fact that AICAR induced a strong YAP phosphorylation (Supplementary Fig. 3c, d). Another AMPK activator, A769662[39], also stimulated YAP phosphorylation in HepG2 cells (Supplementary Fig. 3e). Collectively, our data show that pharmacological activation of AMPK leads to YAP phosphorylation and inhibition, demonstrating a general role of AMPK in YAP regulation.

Energy stress induces both Lats-dependent and -independent YAP phosphorylation

Lats is the major kinase responsible for YAP/TAZ inhibition, although other kinases have also been implicated in their regulation[20, 40, 41]. To confirm the role of Lats in energy stress-induced YAP phosphorylation, we compared the $Lats1^{-/-};Lats2^{fl/fl}$ (Lats1 KO) MEFs with the $Lats1/2^{-/-}$ (Lats1/2 DKO) MEFs[42] generated by infection of the Cre virus in the $Lats1^{-/-};Lats2^{fl/fl}$ (Lats1 KO) MEFs. As expected, deletion of Lats1/2 completely abolished YAP S127 phosphorylation and increased YAP protein levels (Fig. 3a). Moreover, the 2-DG-induced YAP mobility shift was significantly diminished in Lats1/2 DKO MEFs,

supporting a role of Lats in energy-stress-induced YAP phosphorylation. However, 2-DG still induced a visible YAP mobility shift in the Lats1/2 DKO cells (Fig. 3a), suggesting that 2-DG could induce YAP phosphorylation independent of Lats. Interestingly, AMPK activation was noticeably enhanced in the Lats1/2 DKO MEFs compared to Lats1 KO MEFs (Fig. 3a). The enhanced AMPK activation in the Lats1/2 DKO MEFs indicates that these cells are under more severe energy stress. This phenomenon can be explained by a model in which the high YAP activity in the Lats1/2 DKO cells promotes cell growth and increases energy expenditure, thereby reading to energy stress in these cells.

We further investigated the function of Lats in energy stress-induced YAP phosphorylation. Co-transfection of Lats2 increased basal YAP phosphorylation, whereas the Lats2 kinase-inactive (Lats2-KR) mutant blocked YAP phosphorylation (Fig. 3b). Interestingly, Lats2-KR did not completely block 2-DG-induced YAP mobility shift although it strongly reduced 2-DG-induced YAP-S127 phosphorylation, suggesting that 2-DG could also induce Lats-independent phosphorylation of YAP, consistent with the observation in Fig. 3a.

We used the YAP-5SA mutant, which lacks the five known Lats phosphorylation consensus serine residues (including S61, S119, S127, S164, and S381)[13] to investigate the AMPK-dependent but Lats-independent YAP phosphorylation. Transfection of AMPKα, but not the AMPKα DN mutant, induced a mobility shift of the YAP-5SA mutant (Fig. 3c), indicating that AMPK can promote Lats-independent YAP phosphorylation. Energy stress increases the interaction between AMPK and its physiological substrates[43–45]; accordingly, AMPK co-precipitated with YAP and this interaction was further enhanced by 2-DG treatment (Fig. 3d, e). Moreover, the AMPK activators AICAR and metformin increased the association of endogenous YAP and AMPK (Fig. 3f). Although the precise molecular basis for the energy-stress-induced interaction between AMPK and YAP is unknown, our data suggest a direct role of AMPK in YAP phosphorylation.

AMPK inhibits YAP by directly phosphorylating serine 94

To gain mechanistic insight into AMPK-mediated regulation of YAP, we tested whether YAP is a direct substrate of AMPK. AMPK phosphorylated recombinant YAP-WT *in vitro* (Fig. 4a). The YAP-S127A and YAP-5SA mutants were also phosphorylated by AMPK, though more weakly, indicating that AMPK can phosphorylate YAP on residues distinct from the Lats phosphorylation sites. *In vitro* phosphorylation by AMPK altered the migration of YAP-5SA (Supplementary Fig. 4a). Mass spectrometry experiments of several batches of *in vitro* phosphorylated YAP-5SA identified several phosphorylation sites on YAP, including high- and low-confidence sites (Supplementary Fig. 4b). Further *in vitro* phosphorylation experiments confirmed that serine residues 94, 366 and 463 were direct AMPK targets (Fig. 4b and Supplementary 4c). We examined the robustness of YAP as an AMPK substrate by comparing with known physiological AMPK substrates TSC2 and ULK1[43, 44]. AMPK phosphorylated YAP as efficiently as ULK1 (Supplementary Fig. 4d–f); the efficiency of YAP (51–270) phosphorylation by AMPK was comparable with the TSC2 fragment (1300–1367). Because energy starvation or AMPK co-transfection inhibits YAP transcriptional activity (Fig.1d, 2d, 2e), we examined the effect of the putative AMPK phosphorylation sites on YAP activity. Mutation of YAP S94 to glutamate or alanine

diminished the ability of YAP to activate the TEAD1 reporter, whereas mutation of S366 or S463 did not significantly affect YAP activity (Fig. 5a, b). Therefore, we focused our further studies on S94. Notably, substitution of S94 by any residue, including alanine or glutamate, abolished YAP-TEAD interaction (Fig. 5c) and decreased TEAD reporter activity. We propose that phosphorylation of YAP-S94 by AMPK disrupts its interaction with TEAD.

Identification of YAP-S94 as an AMPK phosphorylation site is exciting because our previous studies had demonstrated that YAP-S94 is directly involved in and is essential for the interaction with TEAD[46]. Based on the YAP-TEAD co-crystal structure, YAP-S94 forms a hydrogen bond with Y406 in TEAD[46, 47]. Notably, S94 is functionally conserved from drosophila Yki to mammalian YAP/TAZ and is also predicted to be phosphorylated by PhosphoSite (http://www.phosphosite.org). However, AMPK co-transfection did not inhibit the interaction between YAP and RUNX2 (Supplementary Fig. 4g), suggesting a specific role of S94 phosphorylation in regulating the interaction with TEAD. These observations collectively suggest that AMPK could inhibit YAP function by phosphorylating S94 and disrupting its interaction with TEAD.

We generated a phospho-YAP (S94) specific antibody and confirmed that it selectively recognized *in vitro* phosphorylated YAP, but not unphosphorylated or the S94A mutant of YAP (Fig. 5d). As expected, AMPK transfection or activation of AMPK by AICAR increased YAP S94 phosphorylation (Fig. 5e, 5f). Collectively, our data indicate that AMPK directly phosphorylates YAP on S94 *in vivo* in response to energy stress.

Energy stress inhibits the oncogenic potential of Lats1/2 DKO cells

To further substantiate the Lats-independent regulation of YAP, we measured the expression of YAP target genes in Lats1/2 DKO MEFs. AICAR could still repress the YAP target genes Ctgf and Cyr61, supporting Lats-independent YAP inhibition by energy stress (Fig. 6a). We next examined the role of such Lats-independent YAP inhibition in oncogenic transformation. Lats1/2 DKO MEFs could form colonies in soft agar, an indication of oncogenic transformation (Fig. 6b). YAP/TAZ knockdown blocked the anchorage-independent growth of the Lats1/2 DKO MEFs, suggesting that YAP/TAZ are required for the transforming potential of these cells. Based on our model, AMPK could inhibit YAP in the Lats1/2 DKO MEFs by phosphorylating S94, therefore should suppress the anchorage-independent growth of Lats1/2 DKO MEFs. Indeed, treatment with AICAR or metformin inhibited anchorage-independent growth of Lats1/2 DKO MEFs *in vitro* (Fig. 6c). In an immunocompromised nude mouse xenograft model, injection of Lats1/2 DKO MEFs resulted in tumor development (Fig. 6d). Consistent with the cell culture results, metformin injection significantly reduced xenografted tumor growth in these mice. Collectively, these data support a model that AMPK could inhibit YAP *in vivo* in the absence of Lats1/2.

AMPK is required for YAP inhibition by energy stress

To demonstrate that AMPK mediates the effect of AICAR on YAP inhibition, AMPK was knockdown by siRNA in Lats1/2 DKO MEFs. Knockdown efficiency was confirmed by Western blot (Fig. 7a). Depletion of AMPK blocked the inhibitory effect of AICAR or

A769662 on YAP target gene expression (Fig. 7a and 7b). These results further support that AMPK is involved in YAP inhibition in the Lats1/2 DKO MEFs upon energy stress.

It is possible that AICAR reduced Ctgf/Cyr61 expression and anchorage-independent growth of Lats1/2 DKO MEFs by inhibiting factors other than YAP. Therefore, we tested whether AICAR- or metformin-induced YAP inhibition is important to achieve their tumor-suppressive effects in Lats1/2 DKO MEFs. We generated a YAP construct resistant to AMPK inhibition by fusing the C-terminal transactivation domain of YAP(AD) to TEAD1 fragment residues 1–289, which contains only the DNA binding domain. The TEAD1ΔC-YAP(AD) fusion should be constitutively active and not inhibited by AMPK. When the TEAD1ΔC–YAP(AD) plasmid was expressed in Lats1/2 DKO MEFs, mRNA levels of Ctgf and Cyr61 were not significantly increased, suggesting that activity of the ectopic TEAD1ΔC-YAP(AD) was not significantly higher than the fully activated endogenous YAP/TAZ in the LATS1/2 DKO cells (Fig. 7c). Interestingly, AICAR inhibited the expression of Ctgf and Cyr61 in the vector-transfected cells, but not the TEAD1ΔC-YAP(AD)-expressing cells. Furthermore, AICAR, metformin, and A769662 could not suppress the anchorage-independent growth of the TEAD1ΔC-YAP(AD)-expressing cells, although they suppressed the control group Lats1/2 DKO MEFs (Fig. 7d). These data support a notion that activation of AMPK inhibits the anchorage-independent growth of the Lats1/2 DKO MEFs by suppressing YAP/TAZ activity.

Discussion

Extensive studies have revealed that the Hippo-YAP signalling is regulated by a variety of extracellular signals[48]. These include cell-cell contact signals (such as tight junctions and adherent junctions), physical signals (such as mechanical stress and matrix stiffness), and long-range hormonal signals (such as lysophosphatidic acid and epinephrine). In this study, we show that intracellular metabolic/energy status also regulates Lats and YAP activity. Therefore, the Hippo-YAP pathway can integrate and coordinate both extracellular and intracellular signals.

Cellular energy stress is detected by AMPK, which modulates cellular metabolism and limits cell growth[29]. Our data show that energy stress inhibits YAP via two mechanisms, Lats-dependent and Lats-independent (Fig. 6e). In the former, AMPK may indirectly activate Lats in response to energy stress. Consistently, a recent report has shown that AMPK phosphorylates and stabilizes angiomotin (AMOTL1) to stimulate Lats activity [49]. The Lats-independent mechanism of YAP inhibition is achieved via direct AMPK-mediated phosphorylation of YAP. S94 phosphorylation by AMPK plays a critical role in YAP inhibition by disrupting the YAP-TEAD complex, leading to repression of YAP target genes and inhibition of cell growth. Our previous biochemical and structural studies have defined an essential function of S94 in YAP-TEAD complex formation by forming a hydrogen bond with Y406 in TEAD1[46]. S94 is conserved in TAZ and mutation of the corresponding S51 in TAZ also abolished TAZ-TEAD interaction[50]. Moreover, YAP S94 is also conserved in Yki and mutation of the corresponding S97 abolishes Yki-sd interaction[13]. Therefore, we propose that TAZ and Yki could be similarly regulated by AMPK in response to energy stress, suggesting an evolutionary conserved mechanism of Hippo pathway regulation by

cellular energy status. Our model also indicates that stress-induced AMPK activation can inhibit YAP even in the absence of Lats, providing an additional layer of YAP regulation. Consistent with this notion, AMPK activation inhibits tumorigenesis in Lats1/2 KO cells.

It is worth noting that AMPK can phosphorylate YAP on additional residues, such as S366 and S463. In the accompanying paper from Dr. Chen and colleagues, AMPK-mediated phosphorylation of YAP on S61 inhibits YAP activity[51]. We did not identify S61 as an AMPK phosphorylation site because YAP-5SA mutant, of which S61 was already replaced by an alanine, was used in our in vitro experiments to map the AMPK phosphorylation sites in YAP. However, consistent with the data by Chen and colleagues, we noticed that energy starvation induced a much more dramatic mobility shift of YAP than the YAP-5SA mutant, supporting YAP S61 as one of the AMPK phosphorylation sites. We propose that AMPK has multiple mechanisms to regulate YAP activity in response to varying degrees of energy stress (Fig. 7e). Further evidence supporting a physiological function of the Hippo pathway in cellular energy response is the observation that AMPK activity was dramatically elevated in Lats KO cells (Fig. 3a), indicating that the Lats KO cells are under constant energy stress. Therefore, Lats is likely to play a role in cellular energy homeostasis. Energy stress-induced Lats activation reduces energy expenditure and cell growth, possibly by inhibiting YAP. Our study provides a mechanism of signal integration and crosstalk at YAP through multiple mechanisms of regulation.

Considering the general role of YAP in promoting cell proliferation and inhibiting apoptosis, it is not surprising that YAP activity is negatively regulated by cellular energy stress. When the Hippo pathway is inhibited under favorable conditions of low cell density and high serum (or hormonal signals), such conditions would normally allow YAP activation and cell growth. However, cell proliferation should not proceed if cellular energy is limited. Therefore, the direct inhibition of YAP by AMPK provides a mechanism to ensure that cell proliferation occurs only when favorable growth conditions are available. YAP inhibition by AMPK adds new dimensions to both physiological regulation of YAP and the biology of AMPK in cell growth control. Inhibition of YAP may contribute to the growth inhibitory and tumor suppressing activity of AMPK. Indeed, metformin has significant benefit of reducing tumor incidence and is the most prescribed among all drugs [37]. Inhibition of YAP may contribute to the tumor inhibitory effect of metformin. Thus, pharmacological activation of AMPK may offer a potential therapeutic benefit for cancers with high YAP activity, even in tumors with diminished Lats activity.

METHODS

Antibodies and reagents

Anti-CTGF (sc-14939, 1:500), Cyr61 (sc-13100, 1:500) and donkey anti-goat IgG HRP Santa Cruz (sc-2020, 1:5,000) antibodies were obtained from Santa Cruz Biotechnology. Anti-YAP (#4912, 1:1,000), phospho-YAP (S127) (#4911, 1:1,000) TAZ (#4883, 1:1,000), Lats1 (#3477, 1:1,000), phospho-Lats1/2 (S909/872) (#9157, 1:1,000), phospho-Lats1/2 (T1079/999) (#9159, 1:1,000), MST1 (#3682, 1:1,000), phospho-MST1/2 (T183/180) (#3681, 1:1,000), AMPKα (#2532, 1:1,000) phospho-AMPKα (T172) (#2535, 1:1,000), ACC (#3676, 1:1,000) and phospho-ACC (S79) (#3661, 1:1,000) were obtained from Cell

Signaling. Anti-Lats1 (A300-378A, 1:500) and YAP (A302-309A, 1:500) were obtained from Bethyl Laboratory. Anti-α-Vinculin (V9131, 1:2,000) was obtained from Sigma-Aldrich. Anti-TEF (TEAD1) (610922, 1:500) was from BD Biosciences. Actin (ab3280, 1:5,000) was obtained from Abcam (Cambridge, MA). Alexa Fluor 555-conjugated secondary antibody (A31572, 1:1,000) and Alexa Fluor® 488 Goat Anti-Rabbit IgG (H+L) Antibody (A11008, 1:1,000) were obtained from Invitrogen. Horseradish peroxidase conjugated secondary antibodies (NA931V and NA934V, 1:5,000) were obtained from GE Healthcare. Monoclonal ANTI-FLAG® M2-Peroxidase (HRP) antibody (A8592, 1:5,000) was obtained from Sigma-Aldrich. HA-Tag (6E2) mouse (HRP Conjugate) (#2999, 1:5,000) antibody was obtained from Cell Signaling. Anti-phosphorylated S94 antibody was generated by immunizing rabbits with phosphopeptides (Abbiotec and Gentex, 1:500). The phospho-specific antibodies were affinity purified. Phos-tag conjugated acrylamide was purchased from Wako chemicals. The following chemicals were used in this study: AICAR (#2840), Metformin hydrochloride (#2864), and A769662 (#3336) were purchased from TOCRIS and Toronto research chemicals. 2-Deoxy-D-glucose (D8375) was purchased from Sigma-Aldrich. Recombinant AMPK α/β/γ complex was purchased from GenScript. Mutagenesis was performed based on Quick-Change mutagenesis (Stratagene).

Cell culture and transfection

HEK293A, HEK293P, HEK293T, H2.35, NIH3T3, C2C12, and HeLa cells were cultured at 37 °C in Dulbecco's modified Eagle's medium (DMEM) with 10% fetal bovine serum (FBS) (Invitrogen) and 50 μg/ml penicillin/streptomycin in a humidified incubator with 5% CO_2. MCF10A cells were cultured in DMEM/F12 supplemented with 5% horse serum, 20 ng/ml EGF, 0.5 μg/ml hydrocortisone, 10 μg/ml insulin, 100 ng/ml cholera toxin, and 50 μg/ml penicillin/streptomycin. HepG2 cells were cultured in RPMI1640 supplemented with 10% FBS and 50 μg/ml penicillin/streptomycin. For glucose starvation, cells were washed twice with PBS and then incubated in DMEM without glucose and pyruvate (0 g/L glucose, 0 mM pyruvate; Invitrogen) supplemented with 10% FBS, Dialyzed (Invitrogen). Lats1 KO MEF cells, provided by Dr. Dae-SiK Lim (Korea Advanced Institute of Science and Technology), were maintained in DMEM with 10% FBS [39]. AMPKα WT and AMPKα DKO MEFs, a gift from Dr. Benoit Viollet, were cultured in DMEM medium with 10% FBS [40]. PolyJet™ DNA *In Vitro* Tranfection reagent (SignaGen Lab.) was used for transfection. siRNAs were synthesized by Dharmacon and delivered into cells using RNAiMAX (Invitrogen) according to manufacturer's instructions.

PCR Genotyping

The genomic DNA was extracted from AMPKα WT and DKO MEFs and genotyped by PCR. Independent PCR reactions were assembled for each allele. Detection of AMPKα1 wild-type allele used a sense primer (5'- AGCACAGTACCTGGTATCTTATAGG -3') and AMPKα1 KO allele used a sense primer (5'- ACCAGAAGCGGTGCCGGAAAGCTGG -3'). The antisense primers were specific for the AMPKα1 wild-type allele (5'- GGACTTATTACTAAACAGACCTCTG -3') and the AMPKα1 knockout allele (5'- TGTAGTCGGTTTATGCAGCAACGAG -3'). In the case of AMPKα2, the sense primers used were (5′- GCTTAGCACGTTACCCTGGATGG -3′) for the wild-type allele and (5′- GTTTGTGCTTATCTACTTTGTTTCC -3′) for the AMPKα 1 KO allele. The antisense

primers were (5′- GTCTTCACTGAAATACATAGCA -3′) for the wild-type and (5′-TGTGCTTCCTAACTGCAGATGCAGTG -3′) for AMPKα 1 KO allele. The PCR genotyping was performed with 5ng genomic gDNAs, 3mM each primer, and Biopioneer 2xPCR mastermix according to the manufacture's instruction. DNA bands were separated in a 1% agarose gel, being the sizes of about 329bp for AMPKα1 WT allele, 466bp for AMPKα1 KO allele, 260bp for AMPKα2 WT allele and 600 bp for AMPKα2 KO alleles, respectively.

Mass spectrometry

Samples were run 1cm into an 8–16% SDS-PAGE gel and gel slices excised. A gel band corresponding to the GST-YAP2 fusion protein was cut from a SDS–PAGE gel after an *in vitro* kinase reaction. Proteins in the gel were subjected to in-gel trypsin digestion. The first digested the sample with trypsin and then the extracted peptides are splited into two fractions. One of the those fractions was further digested with thermolysin, a non specific protease. The resulting peptide mixture was subjected Liquid chromatography tandem-mass spectrometry (LC-MS/MS) (Fred Hutchinson Cancer Research Center Proteomics facility). The mass spectrometry data were analyzed by Proteome Discover. Next the phosphopeptides that were identified, were analyzed by a program called PhosphoRS to determine site localization confidence.

Lambda phosphatase treatment

To evaluate the effects of phosphorylation on YAP, the AMPKa WT and DKO cells were treated with 2-DG (1 h) and then harvested.cells were lysed with mild lysis buffer (50 mM HEPES at pH 7.5, 150 mM NaCl, 1% NP-40, 10 mM pyrophosphate, 10 mM glycerophosphate, 50 mM NaF and protease inhibitor cocktail [Roche]), and centrifuged at 12,000 × *g* for 15 min at 4 °C. The supernatants were incubated with either 5U lambda phosphatase (NEB) in the phosphatase buffer

Primary hepatocyte isolation

Mouse primary hepatocytes were isolated according to a method described in [46] with modifications. Briefly, under the perfusion, liver was washed in Ca^{2+} and Mg^{2+}-free EBSS (Invitrogen) with 0.1 mM EGTA and 0.1 mM EDTA, and then digested with HBSS buffer (Invitrogen) containing 0.5 mg/ml collagenase IV and 0.5 mg/ml trypsin inhibitor (Roche). The perfused liver was dispersed and washed with DMEM. Hepatocytes were purified from the liver cells by gradient centrifugation in 50% Percoll (Invitrogen), and washed with DMEM. 1×10^6 hepatocytes were seeded onto each well of 6 well plates in DMEM supplemented with 10% FBS. William Medium E (Invitrogen) was used for the subsequent culture.

Retrovirus infection and stable cell lines

To generate TEAD1ΔC-YAP-AD expressing stable cells, retrovirus infection was performed by transfecting 293 Phoenix retrovirus packaging cells with pPGS empty vector or TEAD1ΔC-YAP(AD); TEAD1-ΔC (1–289) fused with the YAP C-terminal activation domain (290–488) construct. After transfection (48 hr), retroviral supernatant was filtered

through a 0.45-μm syringe filter, and used to infect Lats1/2 DKO MEFs in the presence of polybrene (10 μg/ml, Sigma-Aldrich). Infected cells were selected using G418 (VWR) or hygromycin (Invotrogen) in the culture medium.

Western Blot and immunoprecipitation

Immunoblotting was performed using a standard protocol. The phos-tag reagents were purchased from Wako Chemicals, and gels containing phos-tag were prepared according to the manufacture's instructions. For immunoprecipitation, cells were lysed with mild lysis buffer (50 mM HEPES at pH 7.5, 150 mM NaCl, 1 mM EDTA, 1% NP-40, 10 mM pyrophosphate, 10 mM glycerophosphate, 50 mM NaF, 1.5 mM Na_3VO_4, 1 mM PMSF, 1 mM DTT, protease inhibitor cocktail [Roche]), and centrifuged at 12,000 × *g* for 15 min at 4 °C. The supernatants were incubated with the appropriate antibodies for 2 hr at 4 °C, and protein G or protein A conjugated beads were added in for additional 1 hr. Immunoprecipitates were collected by centrifugation and washed four times with lysis buffer, and proteins were eluted with SDS-PAGE sample buffer.

Preparation of recombinant protein

Escherichia coli BL21 were transformed with bacterial expression constructs (pGEX-KG) containing the indicated genes. The expression of the recombinant GST-fusion proteins within the transformed bacteria was induced by using 0.5 mM isopropyl-β-D-thiogalactopyranoside (IPTG) at 18 °C. Cells were re-suspended in PBS containing 0.5% Triton X-100, 1 mM PMSF and 2 mM β-mercaptoethanol, followed by ultrasonication. The proteins were purified by a single step using glutathione bead according to the manufacturer's protocol (Amersham Bioscience). Purified proteins were dialyzed against 20 mM Tris at pH 8.0, and 10% glycerol. Purified GST–YAP protein (0.5 μg) was used for each AMPK assay.

In vitro kinase assay

To analyze kinase activity, HEK293A cells were harvested and lysed with lysis buffer (50 mM HEPES at pH 7.5, 150 mM NaCl, 1 mM EDTA, 1% NP-40, 10 mM pyrophosphoate, 10 mM glycerophosphate, 50 mM NaF, 1.5 mM Na_3VO_4, protease inhibitor cocktail [Roche], 1 mM DTT, 1 mM PMSF) and immunoprecipitated with anti-indicated antibodies. The immunoprecipitates were washed three times with lysis buffer, followed by once with wash buffer (40 mM HEPES, 200 mM NaCl) and once with kinase assay buffer (30 mM HEPES, 50 mM potassium acetate, 5 mM $MgCl_2$). The immunoprecipitated Lats1 was subjected to a kinase assay in the presence of GST-YAP fusion proteins as substrate. Phosphorylation of YAP was detected by phospho-YAP (S127) antibody. For AMPK kinase assays, purified YAP proteins were incubated with recombinant AMPK α1/β1/γ1 proteins (GenScript). The reaction mixtures were incubated for 30 min at 30°C, terminated with SDS sample buffer, and subjected to SDS-PAGE. Phosphorylation of YAP was determined by phospho-YAP (S94) antibody and ^{32}P-autoradiography·

shRNA

YAP (TRCN0000300325), TAZ (TRCN0000319150) and control shRNA were from Sigma-Aldrich (St. Louis, MO). pMD2.G and psPAX2 were used to produce lentivirus in 293T cells.

siRNA

ON-TARGET plus SMARTpool siRNA oligonucleotides targeting mouse AMPKa1 and AMPKa2 were used (Dharmacon). A nontargeting scrambled siRNA duplex was used as a negative control (5'-CCAUUCCGAUCCUGAUCCG-3') and introduced into cells by transient transfection with RNAiMAX (Invitrogen), in accordance with the manufacturer's instructions

Immunofluorescence Staining

HEK293A cells were seeded on coverslips to appropriate density. After 2-DG treatment, cells were fixed with 4% paraformaldehyde-phosphate buffered saline (PBS) for 15 min and permeabilized with 0.1% Triton X-100 in PBS. After blocking in 2% goat serum and 2% BSA in TBS-T for 30min, cells were incubated with primary antibody diluted in 1% BSA for 1.5 hr. Primary antibodies used were YAP (H-125) from Santa Cruz. After three washes with TBS-T, cells were incubated with Alexa Fluor 488- secondary antibodies (Invitrogen, 1:1000 dilution) for 1hr at room temperature. Slides were then washed three times and mounted with ProLong Gold antifade mountant with DAPI. The stained cells were detected using Olympus FV1000 confocal microscopy. The final images were obtained and analyzed by using confocal microscopy with FLUOVIEW viewer software. Each image is a single Z section at the same cellular level.

Luciferase assay

For luciferase reporter assay, HEK293-T cells were seeded in 12 well plates. Gal4-TEAD1, 5×UAS-Luc reporter, pGL3-CTGF-Luc reporter, pRL reporter and indicated plasmids were co-transfected. After transfection (48 hr), cells were lysed and luciferase activity was assayed using the enhanced luciferase assay kit (Promega) following the manufacturer's instructions. The firefly luciferase activity levels were measured and normalized to Renilla luciferase activity.

Soft agar assay

Each 6-well plate (ultra low attachment) was coated with 2 ml of bottom agar (DMEM containing 10% FBS and 0.7% Difco agar noble). Various Lats1/2 DKO MEFs (3×10^3 cells) were suspended in 1.5 ml of top agar (DMEM containing 10% FBS and 0.4% Difco agar noble) into each well. Cells were incubated for 3 weeks and replaced with fresh medium every three days. Colonies were stained using 0.05% crystal violet.

RNA isolation and real-time PCR

Cells were washed with cold PBS and total RNA was extracted using an RNesay kit (Qiagen) treated with RNA-free DNase. 1 μg of RNA was used for reverse transcription with iScript reverse transcriptase (Bio-Rad). cDNA was then diluted and used for real-time

PCR with gene-specific primers using KAPA SYBR FAST qPCR master mix (Kapa Biosystems) and the 7300 real-time PCR system (Applied biosystems). Relative abundance of mRNA was calculated by normalization to HPRT mRNA. Primers are described in;

HPRT AGAATGTCTTGATTGTGGAAGA/ ACCTTGACCATCTTTGGATTA

CTGF: CCAATGACAACGCCTCCTG/ TGGTGCAGCCAGAAAGCTC

CYR61: AGCCTCGCATCCTATACAACC/ TTCTTTCACAAGGCGGCACTC

Hprt GCAGTACAGCCCCAAAATGG/ ACAAAGTCCGGCCTGTATCCAA

Ctgf: CAA GGA CCG CAC AGC AGT T/ AGA ACA GGC GCT CCA CTC TG

Cyr61: GCTCAGTCAGAAGGCAGACC/ GTTCTTGGGGACACAGAGGA

Xenograft

Nude mice were provided by the UCSD animal core facility and housed in pathogen-free room with 12 hr light/dark cycle. A total of 1×10^6 cells were inoculated into 8 weeks old male nude mice by s.c. injection. After tumor size reaches 2 mm in diameter, the mice were randomly divided into two groups with eight animals. One group was treated with metformin at a dose of 250 mg/kg dayly, and the other group was treated with equal volume of PBS by i.p. injection. 15 days after the first metformin treatment, the mice were euthanized and the tumors were weighed. All the procedures followed the UCSD animal care guidelines.

Statistical analysis

Each experiment was repeated two or three times as mentioned in each figure legend. Data are presented as mean ± s.e.m. All statistical tests were performed using Student's t-test (unpaired, two-tailed), $^{*}P<0.05$, $^{**}P<0.01$, $^{***}P<0.001$. No statistical method was used to predetermine sample size. Investigator were blinded to allocation during experiments and outcome assessment.

Supplementary Material

Refer to Web version on PubMed Central for supplementary material.

ACKNOWLEDGEMENTS

We would like to thank Audrey Hong and Fabian Flores for critical reading of the manuscript. This work was supported by grants from National Institutes of Health (CA132809, EY022611, DEO15964, and CA23100, K.L.G.). C.G.H. is supported by a Postdoctoral Fellowship from the Danish Council for Independent Research | Natural Sciences.

REFERENCES

1. Oh H, Irvine KD. Yorkie: the final destination of Hippo signaling. Trends in cell biology. 2010; 20:410–417. [PubMed: 20452772]
2. Pan D. The hippo signaling pathway in development and cancer. Developmental cell. 2010; 19:491–505. [PubMed: 20951342]

3. Zhao B, Tumaneng K, Guan KL. The Hippo pathway in organ size control, tissue regeneration and stem cell self-renewal. Nature cell biology. 2011; 13:877–883. [PubMed: 21808241]
4. Zhao B, et al. Inactivation of YAP oncoprotein by the Hippo pathway is involved in cell contact inhibition and tissue growth control. Genes & development. 2007; 21:2747–2761. [PubMed: 17974916]
5. Dong J, et al. Elucidation of a universal size-control mechanism in Drosophila and mammals. Cell. 2007; 130:1120–1133. [PubMed: 17889654]
6. Hao Y, Chun A, Cheung K, Rashidi B, Yang X. Tumor suppressor LATS1 is a negative regulator of oncogene YAP. The Journal of biological chemistry. 2008; 283:5496–5509. [PubMed: 18158288]
7. Zhao B, Li L, Tumaneng K, Wang CY, Guan KL. A coordinated phosphorylation by Lats and CK1 regulates YAP stability through SCF(beta-TRCP). Genes & development. 2010; 24:72–85. [PubMed: 20048001]
8. Liu CY, et al. The hippo tumor pathway promotes TAZ degradation by phosphorylating a phosphodegron and recruiting the SCF{beta}-TrCP E3 ligase. The Journal of biological chemistry. 2010; 285:37159–37169. [PubMed: 20858893]
9. Lu L, et al. Hippo signaling is a potent in vivo growth and tumor suppressor pathway in the mammalian liver. Proceedings of the National Academy of Sciences of the United States of America. 2010; 107:1437–1442. [PubMed: 20080689]
10. Cai J, et al. The Hippo signaling pathway restricts the oncogenic potential of an intestinal regeneration program. Genes & development. 2010; 24:2383–2388. [PubMed: 21041407]
11. Lee KP, et al. The Hippo-Salvador pathway restrains hepatic oval cell proliferation, liver size, and liver tumorigenesis. Proceedings of the National Academy of Sciences of the United States of America. 2010; 107:8248–8253. [PubMed: 20404163]
12. Ota M, Sasaki H. Mammalian Tead proteins regulate cell proliferation and contact inhibition as transcriptional mediators of Hippo signaling. Development. 2008; 135:4059–4069. [PubMed: 19004856]
13. Zhao B, et al. TEAD mediates YAP-dependent gene induction and growth control. Genes & development. 2008; 22:1962–1971. [PubMed: 18579750]
14. Halder G, Johnson RL. Hippo signaling: growth control and beyond. Development. 2011; 138:9–22. [PubMed: 21138973]
15. Harvey KF, Zhang X, Thomas DM. The Hippo pathway and human cancer. Nature reviews. Cancer. 2013; 13:246–257. [PubMed: 23467301]
16. Johnson R, Halder G. The two faces of Hippo: targeting the Hippo pathway for regenerative medicine and cancer treatment. Nature reviews. Drug discovery. 2014; 13:63–79. [PubMed: 24336504]
17. Strano S, et al. The transcriptional coactivator Yes-associated protein drives p73 gene-target specificity in response to DNA Damage. Molecular cell. 2005; 18:447–459. [PubMed: 15893728]
18. Lapi E, et al. PML, YAP, and p73 are components of a proapoptotic autoregulatory feedback loop. Molecular cell. 2008; 32:803–814. [PubMed: 19111660]
19. Cottini F, et al. Rescue of Hippo coactivator YAP1 triggers DNA damage-induced apoptosis in hematological cancers. Nature medicine. 2014; 20:599–606.
20. Schlegelmilch K, et al. Yap1 acts downstream of alpha-catenin to control epidermal proliferation. Cell. 2011; 144:782–795. [PubMed: 21376238]
21. Zhao B, et al. Cell detachment activates the Hippo pathway via cytoskeleton reorganization to induce anoikis. Genes & development. 2012; 26:54–68. [PubMed: 22215811]
22. Yu FX, et al. Regulation of the Hippo-YAP pathway by G-protein-coupled receptor signaling. Cell. 2012; 150:780–791. [PubMed: 22863277]
23. Mo JS, Yu FX, Gong R, Brown JH, Guan KL. Regulation of the Hippo-YAP pathway by protease-activated receptors (PARs). Genes & development. 2012; 26:2138–2143. [PubMed: 22972936]
24. Miller E, et al. Identification of serum-derived sphingosine-1-phosphate as a small molecule regulator of YAP. Chemistry & biology. 2012; 19:955–962. [PubMed: 22884261]
25. Yu FX, et al. Protein kinase A activates the Hippo pathway to modulate cell proliferation and differentiation. Genes & development. 2013; 27:1223–1232. [PubMed: 23752589]

26. Dupont S, et al. Role of YAP/TAZ in mechanotransduction. Nature. 2011; 474:179–183. [PubMed: 21654799]
27. Wada K, Itoga K, Okano T, Yonemura S, Sasaki H. Hippo pathway regulation by cell morphology and stress fibers. Development. 2011; 138:3907–3914. [PubMed: 21831922]
28. Sansores-Garcia L, et al. Modulating F-actin organization induces organ growth by affecting the Hippo pathway. The EMBO journal. 2011; 30:2325–2335. [PubMed: 21556047]
29. Hardie DG. AMP-activated protein kinase: an energy sensor that regulates all aspects of cell function. Genes & development. 2011; 25:1895–1908. [PubMed: 21937710]
30. Vassilev A, Kaneko KJ, Shu H, Zhao Y, DePamphilis ML. TEAD/TEF transcription factors utilize the activation domain of YAP65, a Src/Yes-associated protein localized in the cytoplasm. Genes & development. 2001; 15:1229–1241. [PubMed: 11358867]
31. Mahoney WM Jr, Hong JH, Yaffe MB, Farrance IK. The transcriptional co-activator TAZ interacts differentially with transcriptional enhancer factor-1 (TEF-1) family members. The Biochemical journal. 2005; 388:217–225. [PubMed: 15628970]
32. Tian W, Yu J, Tomchick DR, Pan D, Luo X. Structural and functional analysis of the YAP-binding domain of human TEAD2. Proceedings of the National Academy of Sciences of the United States of America. 2010; 107:7293–7298. [PubMed: 20368466]
33. Chan EH, et al. The Ste20-like kinase Mst2 activates the human large tumor suppressor kinase Lats1. Oncogene. 2005; 24:2076–2086. [PubMed: 15688006]
34. Praskova M, Xia F, Avruch J. MOBKL1A/MOBKL1B phosphorylation by MST1 and MST2 inhibits cell proliferation. Current biology : CB. 2008; 18:311–321. [PubMed: 18328708]
35. Knowler WC, et al. Reduction in the incidence of type 2 diabetes with lifestyle intervention or metformin. The New England journal of medicine. 2002; 346:393–403. [PubMed: 11832527]
36. Zhou G, et al. Role of AMP-activated protein kinase in mechanism of metformin action. The Journal of clinical investigation. 2001; 108:1167–1174. [PubMed: 11602624]
37. Evans JM, Donnelly LA, Emslie-Smith AM, Alessi DR, Morris AD. Metformin and reduced risk of cancer in diabetic patients. Bmj. 2005; 330:1304–1305. [PubMed: 15849206]
38. Stambolic V, Woodgett JR, Fantus IG, Pritchard KI, Goodwin PJ. Utility of metformin in breast cancer treatment, is neoangiogenesis a risk factor? Breast cancer research and treatment. 2009; 114:387–389. [PubMed: 18438706]
39. Moreno D, Knecht E, Viollet B, Sanz P. A769662, a novel activator of AMP-activated protein kinase, inhibits non-proteolytic components of the 26S proteasome by an AMPK-independent mechanism. FEBS letters. 2008; 582:2650–2654. [PubMed: 18593584]
40. Zhou D, et al. Mst1 and Mst2 maintain hepatocyte quiescence and suppress hepatocellular carcinoma development through inactivation of the Yap1 oncogene. Cancer cell. 2009; 16:425–438. [PubMed: 19878874]
41. Sorrentino G, et al. Metabolic control of YAP and TAZ by the mevalonate pathway. Nature cell biology. 2014; 16:357–366. [PubMed: 24658687]
42. Kim M, et al. cAMP/PKA signalling reinforces the LATS-YAP pathway to fully suppress YAP in response to actin cytoskeletal changes. The EMBO journal. 2013; 32:1543–1555. [PubMed: 23644383]
43. Inoki K, Zhu T, Guan KL. TSC2 mediates cellular energy response to control cell growth and survival. Cell. 2003; 115:577–590. [PubMed: 14651849]
44. Kim J, Kundu M, Viollet B, Guan KL. AMPK and mTOR regulate autophagy through direct phosphorylation of Ulk1. Nature cell biology. 2011; 13:132–141. [PubMed: 21258367]
45. Budanov AV, Karin M. p53 target genes sestrin1 and sestrin2 connect genotoxic stress and mTOR signaling. Cell. 2008; 134:451–460. [PubMed: 18692468]
46. Li Z, et al. Structural insights into the YAP and TEAD complex. Genes & development. 2010; 24:235–240. [PubMed: 20123905]
47. Chen L, et al. Structural basis of YAP recognition by TEAD4 in the hippo pathway. Genes & development. 2010; 24:290–300. [PubMed: 20123908]
48. Yu FX, Guan KL. The Hippo pathway: regulators and regulations. Genes & development. 2013; 27:355–371. [PubMed: 23431053]

49. DeRan M, et al. Energy Stress Regulates Hippo-YAP Signaling Involving AMPK-Mediated Regulation of Angiomotin-like 1 Protein. Cell reports. 2014; 9:495–503. [PubMed: 25373897]

50. Zhang H, et al. TEAD transcription factors mediate the function of TAZ in cell growth and epithelial-mesenchymal transition. The Journal of biological chemistry. 2009; 284:13355–13362. [PubMed: 19324877]

51. Wang W, et al. AMPK modulates Hippo pathway activity to regulate energy homeostasis. Nature cell biology. 2015 in press.

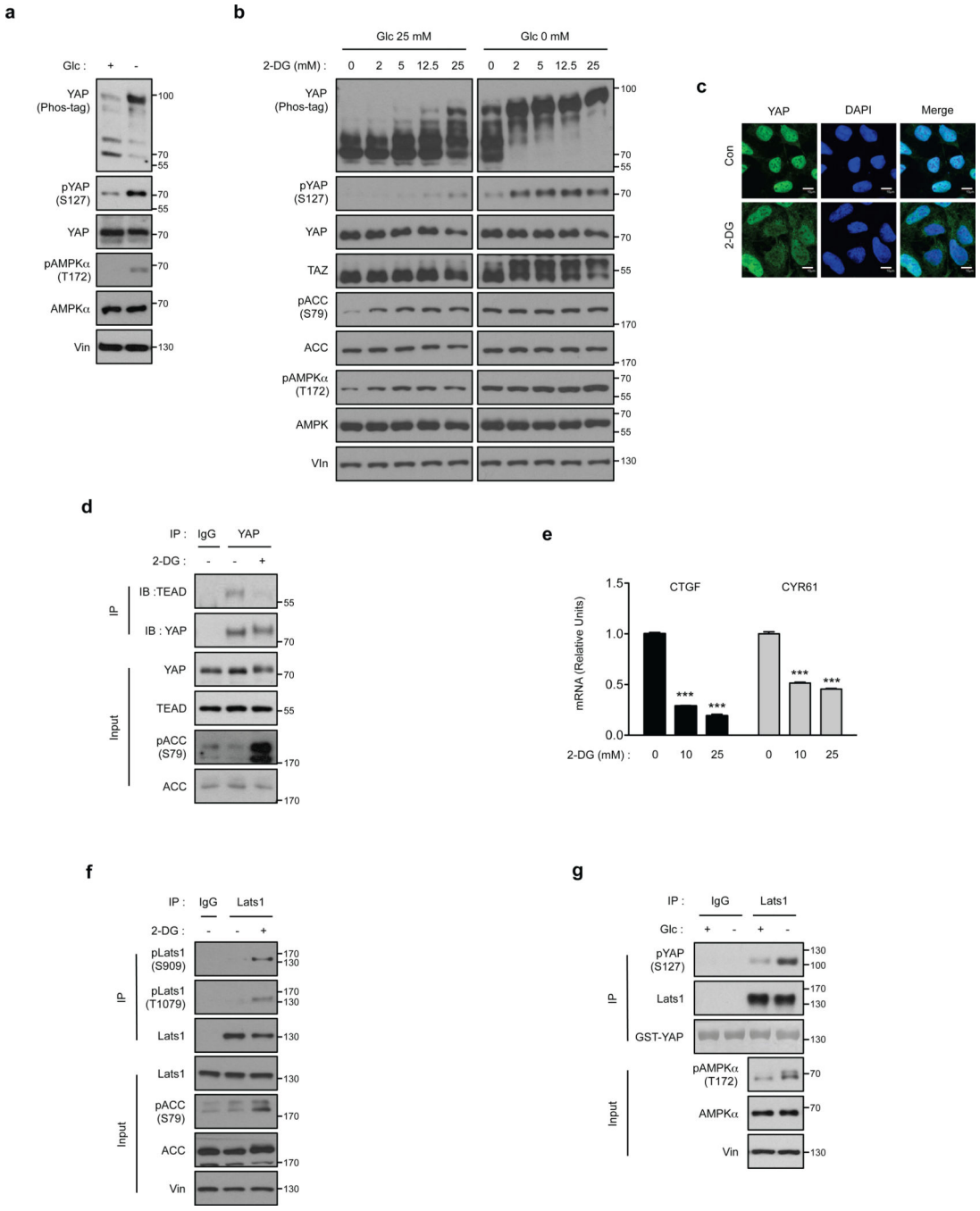

Figure 1. Cellular energy starvation activates Lats and inhibits YAP

(**a**) Glucose starvation induces YAP phosphorylation. HEK293A cells were starved of glucose as indicated for 1 hr. Cell lysates were prepared and subjected to immunoblotting for the indicated proteins and phosphorylation. Phos-tag denotes phos-tag gel used to resolve phosphorylated YAP based on mobility shift. Vin stands for vinculin as a loading control. Protein molecular markers are labeled on the right of each panel. (**b**) 2-DG induces YAP phosphorylation. HEK293A cells were treated with different doses of 2-DG in glucose-rich (25 mM) or glucose-free (0 mM) DMEM medium for 1 hr. Cell lysates were immunoblotted

with anti-AMP-activated protein kinase α (AMPKα), anti-pAMPKα (T172), anti-Acetyl-CoA Carboxylase (ACC), and anti-pACC (S79). Both pAMPKα and pACC were analyzed as indicators of energy starvation. Experiments were similar to panel a. (**c**) 2-DG decreases YAP nuclear localization. HEK293A cells were treated with 25 mM 2-DG for 1 hr. YAP subcellular localization was determined by immunofluorescence staining for endogenous YAP (green); DAPI (blue) was used to stain cell nuclei. Scale Bars, 10μm. (**d**) 2-DG disrupts the interaction between YAP and TEAD1. Cells were treated with 25 mM 2-DG for 2 hr as indicated. Cell lysates were precipitated with YAP or IgG control antibody. Co-immunoprecipitation of TEAD was detected by Western blot. (**e**) 2-DG inhibits YAP target gene expression. HEK293A cells were treated with 10 mM and 25 mM 2-DG for 4 hr, mRNA levels of CTGF and CYR61 were measured by quantitative RT-PCR and normalized to HPRT control (error bars represent ± s.e.m. from n=3 independent experiments). (**f**) Energy stress increased Lats1 phosphorylation. HEK293A cells were treated with 25 mM 2-DG for 1 hr. Endogenous Lats1 was immunoprecipitated and phosphorylation of the activation loop and hydrophobic motif was detected by Western blot with phosphospecific antibodies. (**g**) Glucose starvation activates Lats1 kinase activity. Cells were treated with glucose starvation for 1 hr. Lats1 was immunoprecipitated and *in vitro* kinase assays were performed using recombinant GST-YAP as the substrate. Phosphorylation of GST-YAP was determined by immunoblotting with the phospho-YAP (S127) antibody. All blots and immunofluorescence shown; are representatives of three independent experiments. Uncropped blots are shown in Supplementary Fig. 5. $^{***}P<0.001$, two-tailed *t*-test.

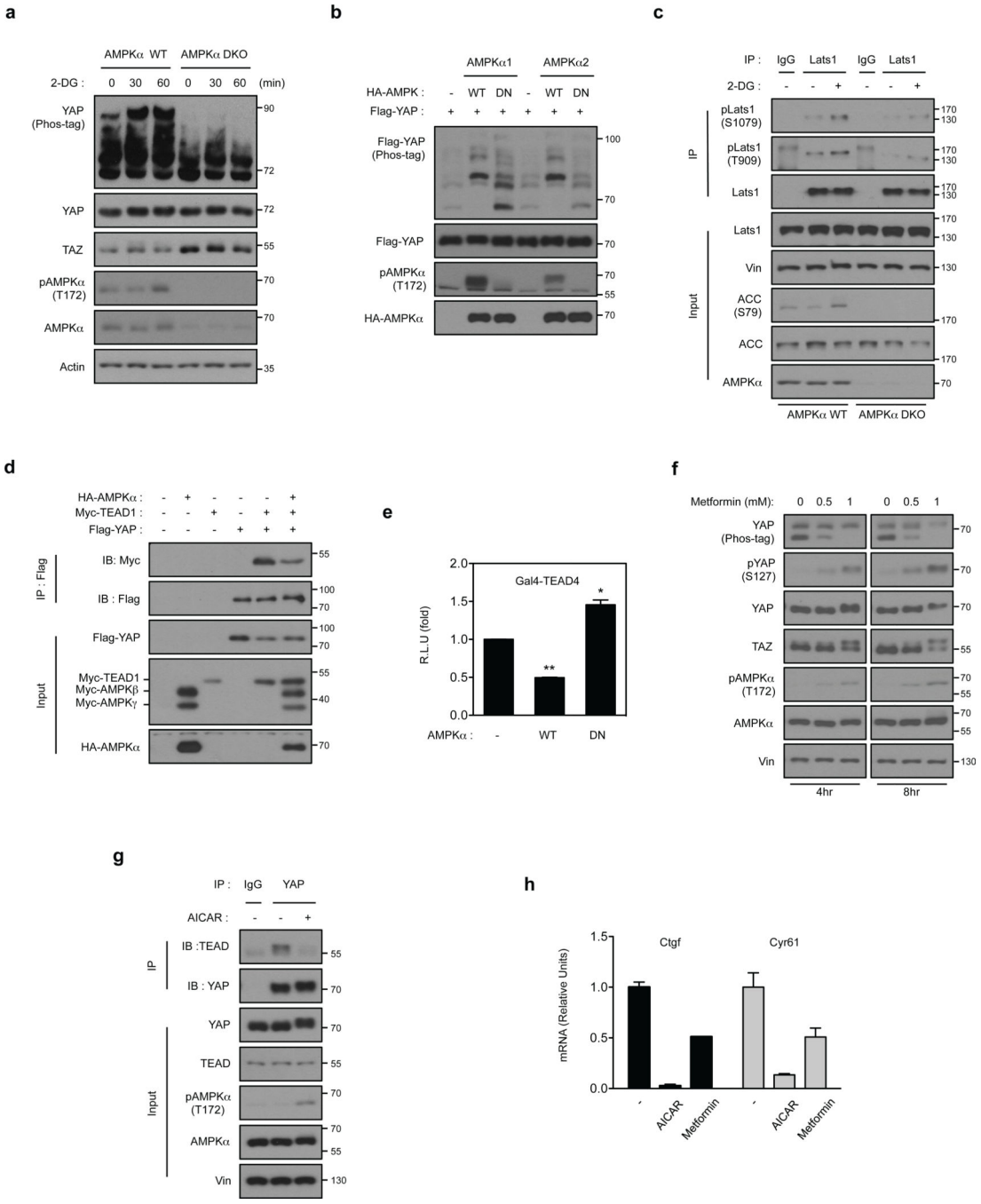

Figure 2. AMPK is required for Hippo-YAP regulation by energy stress

(**a**) The 2-DG-induced YAP phosphorylation depends on AMPK. AMPKα WT and AMPKα DKO MEFs were treated with 25 mM 2-DG for the indicated durations. YAP phosphorylation is determined by phos-tag gel. (**b**) AMPK induces YAP phosphorylation. HEK293A cells were transiently co-transfected with the indicated plasmids as labeled on top of the lanes. Wild type AMPKα (AMPKα WT), but not the kinase-inactive AMPKα (AMPKα DN) increased YAP phosphorylation. (**c**) AMPK is required for Lats1 activation by energy stress. AMPKα WT and AMPKα DKO MEFs were incubated with or without 25

mM 2-DG for 2 hr. Endogenous Lats1 was immunoprecipitated and phosphorylation in both activation loop and the hydrophobic motif was detected by Western blot. (**d**) AMPK disrupts YAP and TEAD1 interaction. HEK293A cells were transiently co-transfected with the indicated plasmids. Flag-YAP was immunoprecipitated and the co-immunoprecipitated Myc-TEAD1 was detected by Myc Western blot. (**e**) AMPK inhibits the TEAD reporter. A luciferase reporter controlled by multiple TEAD binding sequences was transfected in to HEK293A cells together with AMPKα WT or AMPKα DN. After 48 hr, the firefly luciferase activity was measured and normalized to the co-transfected Renilla luciferase internal control (error bars represent ± s.e.m. from n=6 biological replicates). (**f**) Metformin activates AMPK and increases YAP phosphorylation. Primary mouse hepatocytes were treated with different doses of metformin for 4 or 8 hr. Phosphorylation of YAP and AMPK were measured by Western blot. TAZ phosphorylation was indicated by a mobility shift. (**g**) AICAR disrupts YAP and TEAD interaction. Primary mouse hepatocytes were treated with 2 mM AICAR for 4 hr. The endogenous YAP was immunoprecipitated and the co-precipitated TEAD was detected by Western blot. (**h**) AICAR and metformin inhibits YAP target gene expression. Primary mouse hepatocytes were treated with 2 mM AICAR or 2 mM metformin for 4 hr, mRNA levels of Ctgf and Cyr61 were measured by quantitative RT-PCR (error bars represent ± s.e.m. from n=3 independent experiments). All experiments are representatives of three independent experiments except panel e. $^{*}P<0.05$, $^{**}P<0.01$, two-tailed *t*-test.

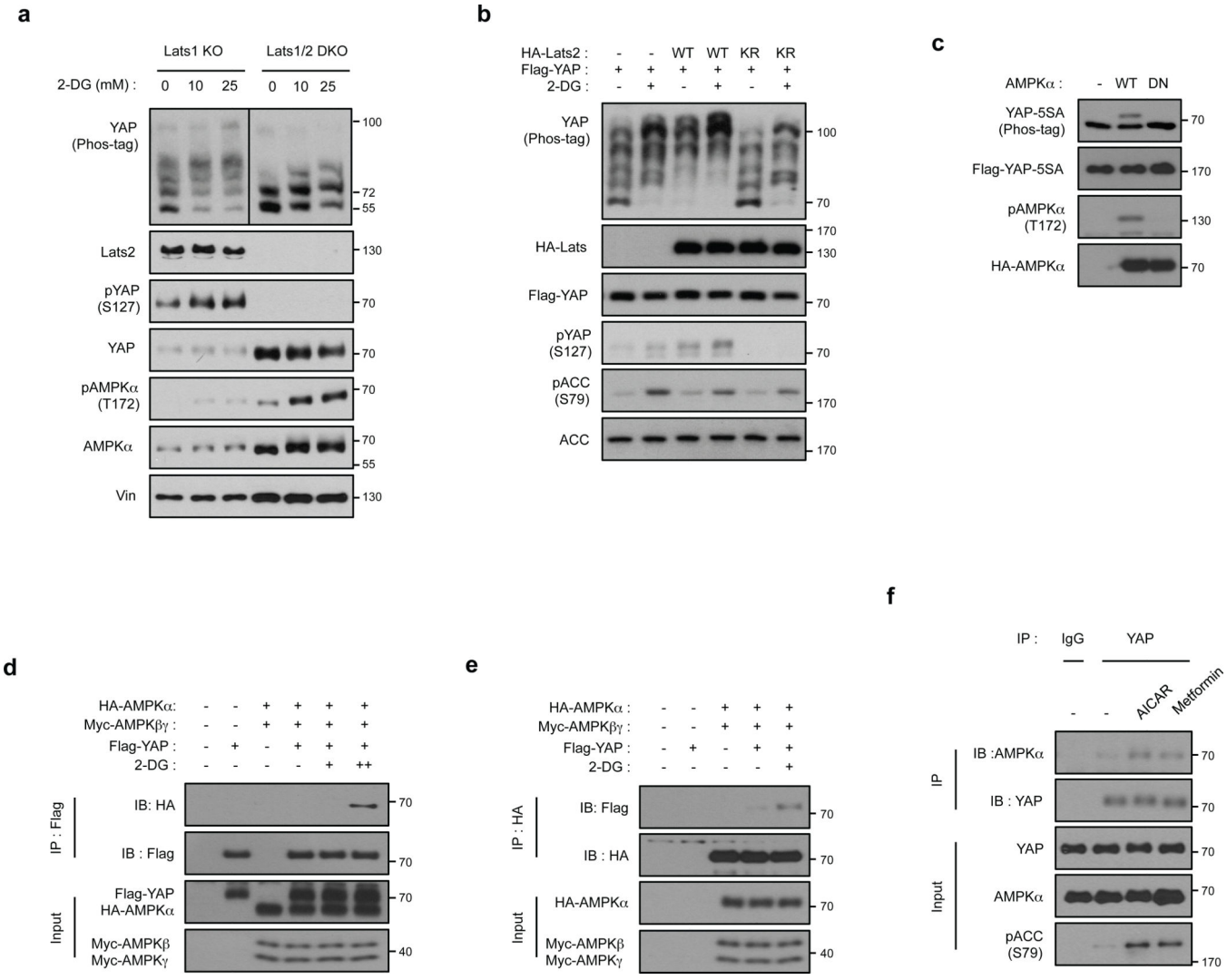

Figure 3. Energy stress induces YAP phosphorylation via both Lats dependent and independent mechanisms

(**a**) Deletion of Lats1/2 diminishes, but not completely abolishes YAP phosphorylation by 2-DG. Lats1$^{-/-}$;Lats2$^{fl/fl}$ (denoted as Lats1 KO) MEFs and Cre- transduced Lats1$^{-/-}$;Lats2$^{fl/fl}$ (denoted as Lst1/2 DKO) MEFs were treated with 10 and 25 mM 2-DG. YAP phosphorylation was detected by phospho-YAP (S127) antibody and phos-tag gel. Lats2 deletion was confirmed by Western blot. All lysates were run on the same gel and the vertical line in YAP phos-tag blot indicated different exposures of the same Western Blot (the YAP phos-tag blot of Lats1/2 DKO samples was exposed shorter due to high YAP protein levels in these samples). (**b**) Overexpressed of kinase-inactive Lats2 (Lats2-KR) abolishes 2-DG-induced S127 phosphorylation, but not total phosphorylation, in YAP. Flag-YAP was co-transfected with Lats2-WT or Lats2-KR mutant. After transfection, cells were treated with 25 mM 2-DG for 1 hr. (**c**) AMPK induces mobility shift of YAP-5SA. Flag-YAP-5SA was co-transfected with AMPKα WT or AMPKα DN in HEK293A as indicated. (**d, e**) 2-DG stimulates the interaction of YAP and AMPKα. HEK293A cells transfected with the indicated plasmids were immunoprecipitated with anti-FLAG (for Flag-YAP) or

anti-HA (for HA-AMPK) and blotted with indicated antibodies for co-immunoprecipitation. (**f**) AICAR or Metformin promotes the association between endogenous AMPK and YAP. H2.35 cells were treated with AICAR or metformin. Cell lysates were immunoprecipitated with YAP or control IgG and Western blotted with AMPKα. All experiments are representatives of three independent experiments except panel e and f. The experiments in e, f were performed two times with similar results.

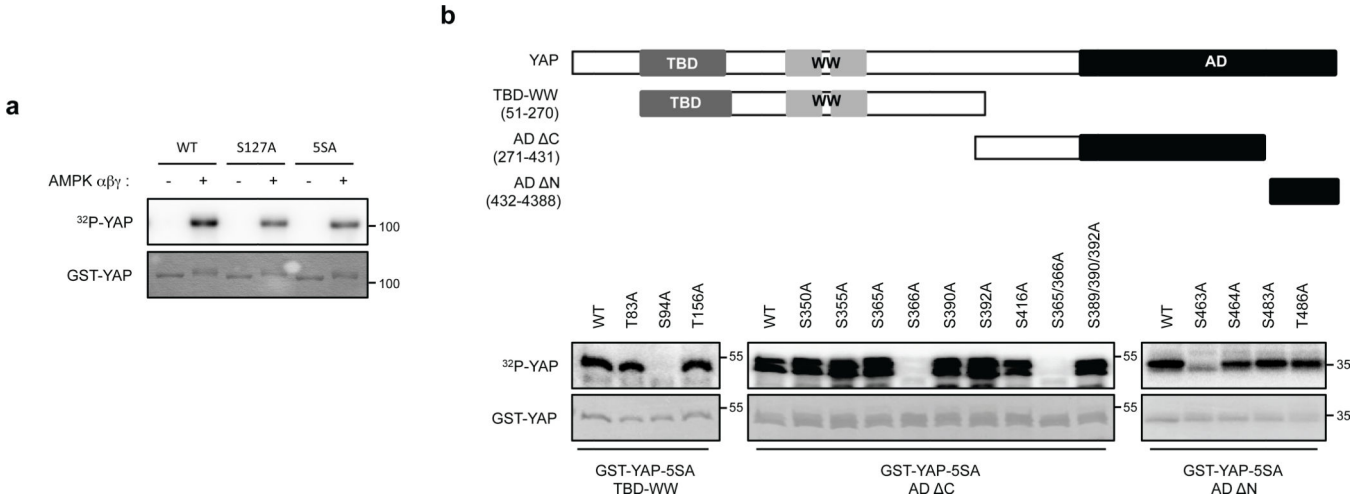

Figure 4. AMPK phosphorylates S94 in YAP

(**a**) AMPK directly phosphorylates YAP *in vitro*. The indicated various YAP mutant proteins were purified from E.coli and used as substrates for *in vitro* phosphorylation by AMPK. Phosphorylation was determined by ^{32}P-autoradiography and the amount of each GST-YAP protein was detected by coomassie staining. (**b**) Confirmation of AMPK phosphorylation sites in YAP by mutagenesis. Schematic representation of YAP domains and deletion constructs used to map phosphorylation sites are shown on the top. The human YAP protein contains a TEAD Binding Domain (TBD; residues 48–102), two WW domains (WW1, 171–204; WW2, 230–263) domains and an Activation Domain (AD; 292–488). Three different YAP deletion constructs and multiple amino acid mutations in these YAP truncations were expressed, purified, and used as substrates for *in vitro* AMPK phosphorylation in the presence of ^{32}P-ATP. Phosphorylation was detected by autoradiography. GST-YAP fragment protein was detected by Coomassie staining.

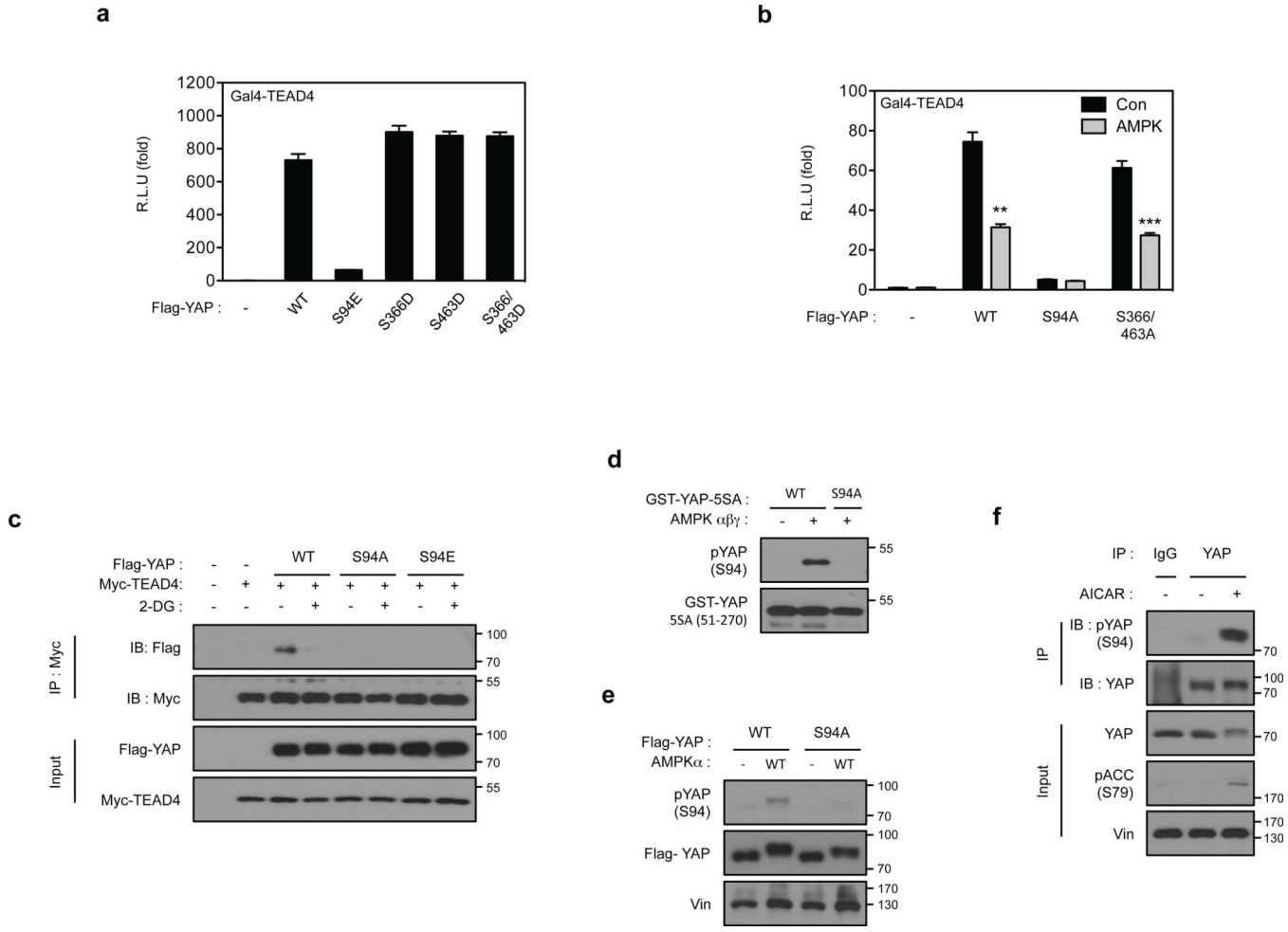

Figure 5. AMPK inhibits YAP activity through phosphorylation of serine 94

(**a**) Phosphomimetic mutant of YAP S94 abolishes YAP activity. The indicated plasmids were co-transfected with a 5×UAS-luciferase reporter for Gal4-TEAD4 and Renilla construct into HEK293T cells. The firefly luciferase activity levels were measured and normalized to Renilla luciferase activity levels (error bars represent ± s.e.m. from n=6 biological replicates). (**b**) S94 is important for YAP activity and inhibition by AMPK. All three AMPK phosphorylation sites in YAP were mutated to alanine. The YAP plasmids were co-transfected with the 5xUAS-luciferase reporter for Gal4-TEAD4 into HEK293T cells together with the control Renilla luciferase. After 48 hr, the firefly luciferase activity was measured and normalized to the co-transfected Renilla luciferase internal control (error bars represent ± s.e.m. from n=6 biological replicates). (**c**) S94 of YAP is essential for 2-DG-induced disruption of YAP-TEAD complex. HEK293A cells were transiently co-transfected with the indicated plasmids followed by treatment with 2-DG. Interaction between Flag-YAP and Myc-TEAD4 was determined by co-immunoprecipitation. (**d**) Evaluation of phospho-specific antibodies for YAP S94 phosphorylation. Phosphoantibody was prepared by immunizing rabbits with synthetic phosphopeptides containing phospho-YAP S94. Recombinant GST-YAP (51–270) fragment was purified from bacteria and phosphorylated by AMPK *in vitro*. After the reaction, 5 ng of the GST-YAP protein was

detected by phospho-YAP S94 or GST antibody. The non-phosphorylatable mutant, GST-YAP-S94A was used as a negative control. (**e**) AMPK increases YAP S94 phosphorylation in transfected cells. Flag-YAP WT and YAP-S94A mutant were transfected into HEK293 cells with or without AMPK as indicated. Flag-YAP was immunoprecipitated and phosphorylation of S94 was detected by the pYAP(S94) phosphoantibody. (**f**) AICAR increases YAP S94 phosphorylation *in vivo*. Primary hepatocytes were treated with 2 mM AICAR for 4 hr. YAP was immunoprecipitated and phosphorylation of S94 was detected by the pYAP(S94) phosphoantibody. All blots shown are representatives from three independent experiments except panel e. $^{**}P<0.01$, $^{***}P<0.001$, two-tailed *t*-test.

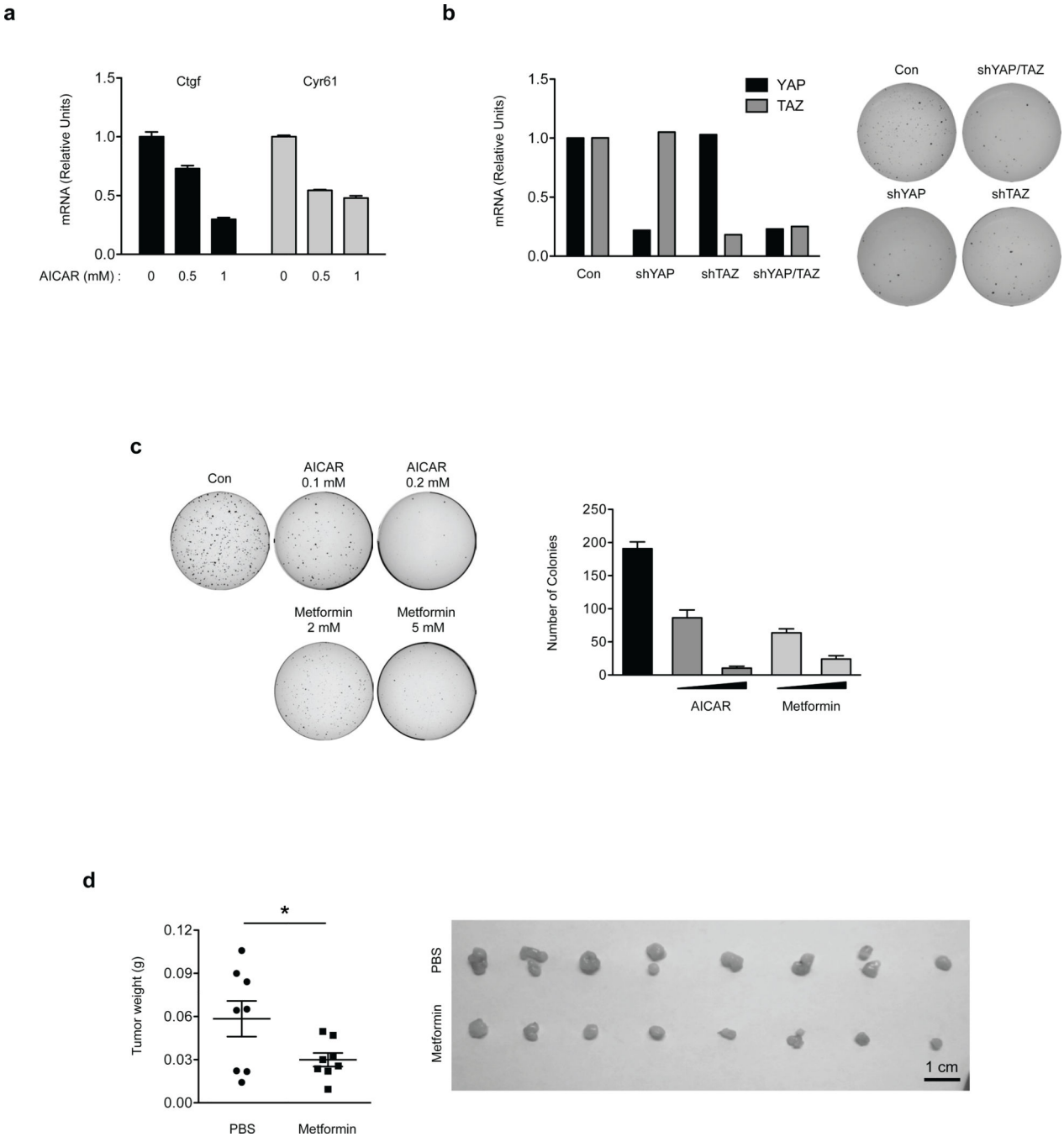

Figure 6. Energy stress attenuates tumorigenecity of Lats1/2 DKO MEFs

(**a**) AICAR inhibits YAP target gene expression in Lats1/2 DKO MEFs. Lats1/2 DKO MEFs were treated with 0.5 mM and 1 mM of AICAR for 5 hr. mRNA levels of Ctgf and Cyr61 were measured by quantitative RT-PCR (error bars represent ± s.e.m. from n=3 independent experiments). (**b**) Knockdown of YAP or TAZ attenuates anchorage-independent growth of Lats1/2 DKO MEFs. YAP or TAZ was knockdown by shRNAs in Lats1/2 DKO MEFs (the experiments was repeated 2 times). The Lats1/2 DKO MEFs (3×10^3 cells) were seeded onto a culture medium containing 0.3% agar and incubated at 37 °C

for 2 weeks. The colonies were stained with 0.005% crystal violet. (**c**) Energy stress attenuates anchorage-independent growth of Lats1/2 DKO MEFs. Lats1/2 DKO MEFs (3×10^3 cells) were seeded onto a culture medium containing 0.3% agar and incubated at 37 °C for 2 weeks. The colonies were stained with 0.005% crystal violet and quantified. AICAR and metformin treatments were indicated (error bars represent ± s.e.m. from n=3 independent experiments). (**d**) Metformin inhibits tumor growth of Lats1/2 DKO MEFs in xenografted mice. Mice were ectopically implanted with $1x10^6$ cells on the both sides of each mouse. Daily i.p. injection of 250mg/kg dose of Metformin or equal volume (300μL) of vehicle (PBS) for 15 days. At the end of the experiment, mice were sacrificed 16 days after implantation and tumor weight was measured (error bars represent ± s.e.m. from 8 tumors (4 mice) per group). Scale bar, 1cm. $^*P<0.05$, two-tailed *t*-test.

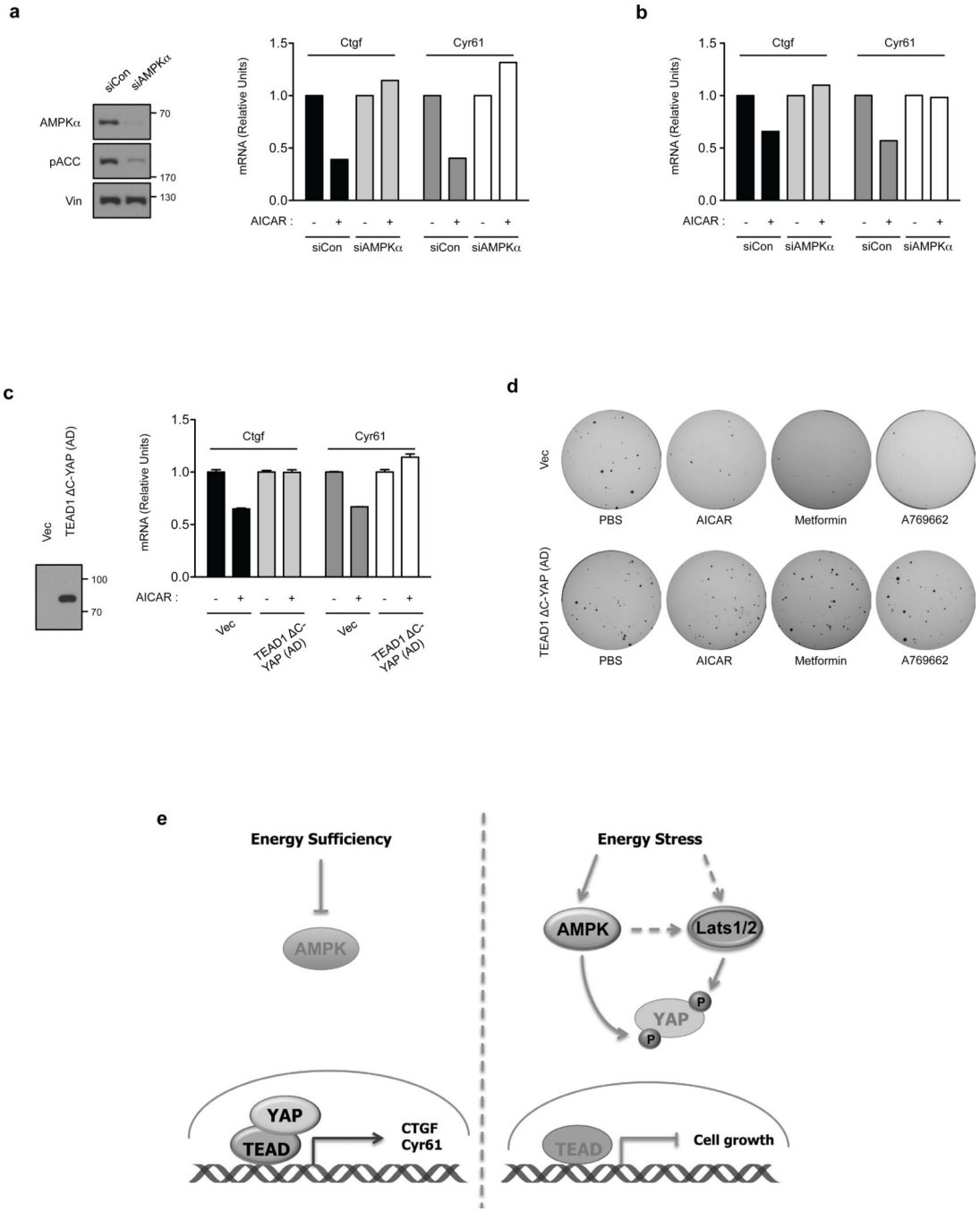

Figure 7. AMPK is required for energy stress to inhibit YAP activity

(**a**) AMPK is required for inhibition of Ctgf and Cry61 by AICAR. Lats1/2 DKO MEFs were transfected with control or AMPK siRNAs. The knockdown efficiency of AMPK was confirmed by Western blot (left panels). After treating with the AMPK activator AICAR (0.5 mM), mRNA levels of Ctgf and Cyr61 were measured by quantitative RT-PCR. The mRNA relative unit values are normalized to 1 (controls without AICAR treatment) (the experiments was repeated 2 times). (**b**) Lats1/2 DKO MEFs were transiently transfected with control (siCon) or AMPK (siAMPKa) siRNA. After treating with the AMPK activator

A769662 (0.3mM for 4 hr), mRNA levels of Ctgf and Cyr61 were measured by quantitative RT-PCR (the experiments was repeated 2 times). (**c**) AICAR cannot inhibit YAP target genes in cells expressing TEAD1ΔC-YAP(AD). HA-TEAD1ΔC-YAP(AD), which is a fusion of the TEAD DNA binding domain with the YAP transactivation domain, was stably expressed in Lats1/2 DKO MEFs. Expression of HA- TEAD1ΔC-YAP(AD) was confirmed by Western blot. Cells were treated in AICAR as indicated and mRNA levels of Ctgf and Cyr61 were measured by quantitative RT-PCR (error bars represent ± s.e.m. from n=5 independent experiments). (**d**) Expression of HA-TEAD1ΔC-YAP(AD) confers Lats1/2 DKO MEFs resistant to growth inhibition by AMPK activators. Soft-agar colony-formation assay was performed with Lats1/2 DKO MEFs expressed with vector (top row) or HA-TEAD1ΔC-YAP(AD) (bottom row). Treatments with PBS control, AICAR, metformin, or A769662 are indicated. (**e**) A model for regulation of Hippo-YAP pathway by energy stress and AMPK. When the energy is sufficient, AMPK is inactive and YAP is active. When cellular energy level is low (energy stress), Both AMPK and Lats are active. The active AMPK and Lats inhibit YAP by phosphorylation.